Aalborg Universitet

Investigation on the Effect of Drained Strength when Designing Sheet Pile Walls

Iversen, Kirsten Malte; Nielsen, Benjaminn Nordahl; Augustesen, Anders Hust

[Link to publication from Aalborg University](#)

Investigation on the Effect of Drained Strength when Designing Sheet Pile Walls

K. M. Iversen
B. N. Nielsen
A. H. Augustesen

AALBORG UNIVERSITY

Department of Civil Engineering

Aalborg University
Department of Civil Engineering
Division of Water and Soil

DCE Technical Report No. 93

Investigation on the Effect of Drained Strength when Designing Sheet Pile Walls

by

K. M. Iversen
B. N. Nielsen
A. H. Augustesen

June 2010

Scientific Publications at the Department of Civil Engineering

Technical Reports are published for timely dissemination of research results and scientific work carried out at the Department of Civil Engineering (DCE) at Aalborg University. This medium allows publication of more detailed explanations and results than typically allowed in scientific journals.

Technical Memoranda are produced to enable the preliminary dissemination of scientific work by the personnel of the DCE where such release is deemed to be appropriate. Documents of this kind may be incomplete or temporary versions of papers—or part of continuing work. This should be kept in mind when references are given to publications of this kind.

Contract Reports are produced to report scientific work carried out under contract. Publications of this kind contain confidential matter and are reserved for the sponsors and the DCE. Therefore, Contract Reports are generally not available for public circulation.

Lecture Notes contain material produced by the lecturers at the DCE for educational purposes. This may be scientific notes, lecture books, example problems or manuals for laboratory work, or computer programs developed at the DCE.

Theses are monograms or collections of papers published to report the scientific work carried out at the DCE to obtain a degree as either PhD or Doctor of Technology. The thesis is publicly available after the defence of the degree.

Latest News is published to enable rapid communication of information about scientific work carried out at the DCE. This includes the status of research projects, developments in the laboratories, information about collaborative work and recent research results.

Investigation on the Effect of Drained Strength when Designing Sheet Pile Walls

K. M. Iversen[1], B. N. Nielsen[2] and A. H. Augustesen[3]

Aalborg University, June 2010

Abstract

Long sheet pile walls are constructed in the cities as an integrated part of deep excavations for e.g. parking lots, pumping stations, reservoirs, and cut and cover tunnels. To minimise costs, the strength of the soil needs to be determined in the best possible way. The drained strength of clay expressed by c' and φ' is often estimated as $c'_{10\%} = 10\% \cdot c_u$, and found by estimations based on the soil describtion, respectively. However, due to possible slicken slides and tension cracks, $c' = 0$ is used on the back side of the sheet pile wall. This reduces the strength significantly. A parametric study is made on the effective cohesion to investigate the influence of c' when designing sheet pile walls. Aalborg Clay is used as a case material. The parametric study is made in both a commercial finite element program and by use of Brinch Hansen's earth pressure theory. In both studies, the analyses are made based on soil pressures only. The finite element analyses show that the safety factors increase with increasing cohesion. The safety factor is defined as the ratio of the surface load applied on the back side to the surface load applied at failure. Brinch Hansen's earth pressure theory indicates that the height, anchor force, and the maximum bending moment in the wall can be lowered significantly when the effective cohesion is increased above zero. However, as the cohesion increases, the drop in the moment levels off, which implies that the benefit obtained from investigations increasing the cohesion more than $c'_{10\%}$ is small.

1   Introduction

Sheet pile walls are generally used in quay constructions and temporary work applications. In the later years, an increasing number of underground constructions have been established in the cities. The depth of the excavation is increasing, which causes problems for the engineers; they need to design increasingly longer retaining walls to make deep excavations possible.

When designing sheet pile walls in clay, both the short and long-term condition must be considered. In the long-term condition, the undrained strength of the clay is applied. The undrained strength is normally estimated from the insitu vane test conducted together with the normal site investigation.

The short-term condition is investigated by applying a drained strength to the soil, which for clay generally implies an effective internal angle of friction φ' and an effective cohesion c'. These parameters can be found by a triaxial test. However, these tests are both time consuming and expensive.

To overcome this, the drained strength parameters are often estimated. The effective cohesion is generally found as $c'_{10\%} = 10\% \cdot c_u$, while φ' is estimated from the soil description.

---

[1]Graduate Student, Dept. of Civil Engineering, Aalborg University, Denmark.

[2]Assistant Professor, M.Sc., Dept. of Civil Engineering, Aalborg University, Denmark.

[3]Specialist in Geotechnical Engineering, Ph.D., M.Sc., COWI A/S. Part-time lecturer, Dept. of Civil Engineering, Aalborg University

The soil might have slicken slides or be fissured due to tension in the soil, and these characteristics will reduce the soil strength. These tension cracks will especially be present on the back side of a sheet pile wall. Normal Danish practice is to let the effective cohesion be zero on the back side, from surface level to excavation level. Here, excavation level is the level to which the soil is removed on the front side of the sheet pile wall.

The effective cohesion is normally set as zero on the back side of the wall for design purpose of all sheet pile walls, independent on the depth of the tension cracks. The purpose of this paper is to investigate the benefits obtained if an effective cohesion of $c'_{10\%}$ is applied on the back side of the wall. Further, it is tried to evaluate the benefits obtained if cohesions larger than $c'_{10\%}$ are applied.

As a case study, sheet pile walls in Aalborg Clay are investigated. The strength of Aalborg Clay is defined by Iversen et al. (2010), and the results concerning constants value of $c'_k = 13kPa$, $\varphi'_k = 28.1^o$ and $c_{uk} = 100.8kPa$ are used. The drained strength is found by use of the MIT-plot (Lade, 2003), for which reason this material is referred to as the MIT-material.

The depth of a tension crack is calculated in the drained state to $4.3m$ (Dansk Ingeniørforening, 1984). The case study considers both a free and an anchored wall. The excavation level is $5m$ for the free wall and $12m$ for the anchored wall. Using $c' = 0$ on the back side to excavation level due to tension cracks is a very conservative estimate for the anchored sheet pile wall.

Two cases of sheet pile walls are investigated (i) one where the soil surrounding the wall is defined as a homogeneous, non-layered soil and (ii) one where the drained shear strength is set equal to zero on the back side of the wall from the surface to excavation level. Both these cases are investigated for a free and an anchored wall, which give four cases in total. All cases are investigated for soil pressures only, as the models are constructed with no difference in water pressure between the front and the back side of the sheet pile wall.

2 Numerical Model

The numerical analyses are made by use of the commercial FEM program PLAXIS v. 9.02 (PLAXIS b.v., 2010). The models are all based on a similar geometrical model. The overall geometry can be seen in Fig. 1. The horizontal and vertical dimensions of the model are $45m$ and $40m$, respectively.

The dimensions of the model are chosen so that the failure mechanism for the sheet pile wall will be unaffected by any boundaries. Furthermore, the horizontal width is chosen so that the extension of the surface load behind the sheet pile wall can be considered infinite. The vertical width is chosen so it is possible to maintain the overall geometry even for long sheet pile walls.

Standard fixities are applied to the boundaries of the model. According to Brinkgreve (2008) this implies $u_x = 0$ for geometry lines with the lowest and highest x-value and $u_x = u_y = 0$ for the geometry line with the lowest y-value.

The model is constructed as a plane strain model. The acceleration in the y-direction is set to $9.8m/s^2$, i.e. normal gravity is used.

The mesh is constructed by 15-node triangular elements. The global coarseness of the mesh is chosen to "medium" in all models, which is shown to be sufficient in an analysis of convergence. Furthermore, the mesh around the sheet pile wall is refined once. These settings of the mesh provides between 316 and 431 elements. The model containing most elements is the anchored sheet pile wall with $c' = 0$ on the back side to excavation level. Fewest elements are found in the non-layered model of a free sheet pile wall.

2
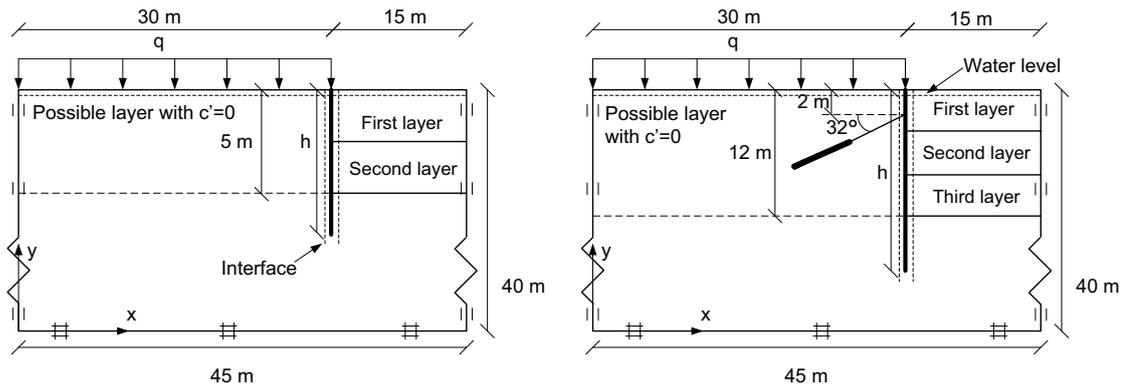
Figure 1: The PLAXIS models for the parametric analyses on the free and the anchored sheet pile wall, respectively.

The ground water level is placed in level with the surface before excavation on the front and back side. This placement is kept after excavation, and in this way the analyses are made only regarding the soil pressure and do not include any difference in water pressure or gradients due to ground water flow.

The sheet pile wall is modelled to be very stiff compared to the soil material. In this way, failure does not occur due to large deformations of e.g. the top of the wall. The properties for the sheet pile wall can be seen in Tab. 1. To avoid reduction of the normal stiffness, Poisson's ratio is set equal to zero (Brinkgreve, 2008).

Table 1: Input parameters for the sheet pile wall.

Type of material	Elastic
Normal stiffness	$7.5 \cdot 10^6 kN/m$
Flexural rigidity	$1.0 \cdot 10^6 kNm^2/m$
Equivalent thickness	$1.265m$
Weight	$10kN/m/m$
Poisson's ratio	0

To model the soil-to-wall interaction, interfaces are placed around the wall. To avoid any high peaks in stresses and strains, the interface is extended $1m$ below the wall (Brinkgreve, 2008). Generally, the interface is assigned the same properties as the surrounding soil layers, where the reduction factor for the strength of the interface R_{inter} is set to 0.67. However, the strength of the extended part should not be reduced due to a manual setting for R_{inter}, and a special ma-

terial is assigned to the extension. The settings correspond to the surrounding soil material but with R_{inter} set as rigid.

Two different soil materials are defined: one corresponding to the strength found by Iversen et al. (2010) (MIT-material) and one calibrated to a load-displacement curve from a triaxial test on Aalborg Clay, using the "soil-test"-modulus in PLAXIS. A triaxial test from the Friis project, described by Iversen et al. (2010), is used to calibrate the material settings.

Both the stiffness, the unit weight, and the permeability are of minor importance as the analyses are made with respect to failure only and do not include ground water flow. For the MIT-material, all these parameters are estimated. For the calibrated material only the unit weight and the permeability are estimated as the stiffness is calibrated to be E_{50}, according to the triaxial load-displacement curve. The defined materials can be seen in Tab. 2. The materials defined in this table are referred to as the original materials.

In addition to these materials, two materials are defined as cohesionless. Both materials are based on those described in Tab. 2 and only the cohesion is changed to $c' = 0.2kPa$ as it is recommended not to use $c' = 0$ in PLAXIS (Brinkgreve, 2008). However, using $c' = 0.2kPa$ still leads to the cohesion being much smaller and close to zero compared to the other materials, and it is therefore fair to

3

Table 2: Input parameters for the soil material.

	MIT-material	Calibrated material
Model type	Mohr-Coulomb	Mohr-Coulomb
Behaviour	Drained	Drained
γ_{unsat} $[kN/m^3]$	17	17
γ_{sat} $[kN/m^3]$	20	20
k_x $[m/day]$	0.001	0.001
k_y $[m/day]$	0.001	0.001
E_{ref} $[kPa]$	20000	28000
v $[-]$	0.3	0.3
c' $[kPa]$	13	9
φ' $[^o]$	28.1	28.7
ψ $[^o]$	0	0
R_{inter} $[-]$	0.67	0.67

consider these materials to be cohesionless.

The anchor is modelled as an inclined soil anchor with an inclination of 32° with horizontal. The free and the fixed length is 9.4m and 5.8m, respectively. The free part is modelled as an elastic anchor rod with a Young's modulus of $2 \cdot 10^5 kN$. The fixed part is modelled as a geogrid with a Young's modulus of $1 \cdot 10^5 kN$. The anchor is pre-stressed to 200kN/m. In this way, failure will be due to insufficient soil strength and not due to large deformations of the top of the sheet pile wall.

The calculation is defined as staged construction phases succeeded by safety calculations. The staged construction is made to match a true excavation process; the surface load is applied and the sheet pile wall is installed. Hereafter the layers are removed from top towards the bottom. In the anchored model, the anchor is placed and pre-stressed in the stage after the first layer is removed, cf. Fig. 1.

Two safety calculations are applied. The first $SF_{\varphi-c}$ calculates the safety as the strength in the soil to the critical strength at failure, i.e. a reduction of both φ' and c' is introduced. The second SF_{Mload} defines the safety factor as the working load to the failure load, i.e. the surface load is increased and involves no change in the strength parameters. Increasing the surface load is done by the $\sum M_{load}$ function in PLAXIS.

Before using the $\sum M_{load}$ function it is

tested for the following: (i) failure (magnitude of the failure load and the shape of the failure mechanism) must match what can manually be obtained by increasing the surface load, (ii) SF_{Mload} must converge towards results obtained for the φ-c reduction, and the curve must be smooth, i.e. lower safety factors must be obtained for higher values of the input load, and (iii) the results must be considered independent of the input parameters for the $\sum M_{load}$-function.

For a free sheet pile wall, safety factors obtained by the ΣM_{load}-function give smooth convergence curves. The failure load is only vaguely dependent on the input values, when the input value varies from $5 - 20kN/m$ higher than the reached value. For higher input values, the reached value differs.

For an anchored sheet pile wall it is observed that the ΣM_{load} function is more stable compared to the free sheet pile wall. For the free walls, collapse of the soil body is observed to occur due to deformations in the top of the wall. This is prevented in the anchored models where the anchor minimises the deformations in the top of the wall. A thesis is that collapse of the soil body due to this occurs in a more distinct way, compared to the free wall. However, this thesis has not been proved.

The failure loads calculated as $q_{input} \cdot \sum M_{load}$ are found to be constant for varying input of the surface load. Only for one value of the input load, the failure load is found to be remarkably low. No explanation is found for this outcome. Further, the failure load is less dependent on the input load compared to the free sheet pile wall.

Table 3: Overview of the eight models.

Free wall	Non-layered	MIT-material
		Calibrated material
	$c' = 0$	MIT-material
		Calibrated material
Anchored wall	Non-layered	MIT-material
		Calibrated material
	$c' = 0$	MIT-material
		Calibrated material

Eight models are investigated in total, cf. Tab. 3, with the geometry as seen in Fig. 1 and the material settings as seen in Tab. 2.

3 Results

The "Parametric Variation"-function described by Brinkgreve (2008) is used to conduct the parametric analyses of the effective cohesion. First, the length of a sheet pile wall in the given soil conditions is found by means of SPOOKS (GEO, 2010). Hereafter the FEM-model is constructed with the given height of the wall. However, to be able to compare the results, one length is chosen for each model type.

When the geometry of the model is made, the stability is verified for each model as described for the $\sum M_{load}$-function, cf. Section 2. Generally, all models show stability towards the total multiplier function. However, the free sheet pile wall is somewhat less stable, especially for the models concerning the calibrated material, where the progress of the calibration curve is found to be different and the results are found to depend on the input value to $\sum M_{load}$.

In this analysis PLAXIS is previously found to be unstable, when calculations are performed on constructions far from failure. The input for the surface load is therefore

chosen so that $SF_{\varphi-c} \approx 1.2$, which according to EN1997-1 DK NA:2008 is the partial coefficient introduced for drained soil strength (European Committee for Standardization, 2008). To ease the comparison of the results, the models could have been built with matching surface load, but this might cause problems when conducting the parametric analysis as some constructions would be far from failure.

A brief review of the results can be seen in Tab. 4. Generally, it is found that the MIT material provides a safer construction, as more surface load can be applied to obtain the same $SF_{\varphi-c}$. This can be explained by the difference in strength parameters, where the MIT-material has a 30% higher cohesion but only a 2% lower internal angle of friction. Furthermore, it is found that the non-layered case has a higher safety factor compared to the case with $c' = 0$ on the back side to excavation level.

The parametric analysis is conducted for the eight models, cf. Tab. 3. First results are presented for the free sheet pile wall, cf. Fig. 2. The results obtained by the $\sum M_{load}$-function are used to see the variation of the safety factor with increasing effective cohesion within each model, and for all four models SF_{Mload} is found to increase linearly with increasing cohesion.

Some deviation from the linear variation is found for the models with $c' = 0$ to excavation level, when the cohesion is raised to $10 -$
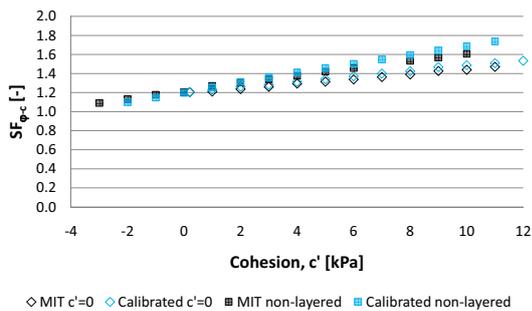
Table 4: Results from the parametric analysis.

		MIT	Calibrated
Free (non-layered)	$q[kN/m^3]$	45	30
$h = 8m$	$SF_{\varphi-c}$	1.2025	1.1971
	SF_{Mload}	1.5939	1.4296
Free ($c' = 0$)	$q[kN/m^3]$	35	27
$h = 9.5m$	$SF_{\varphi-c}$	1.2049	1.2037
	SF_{Mload}	1.7837	1.7254
Anchored (non-layered)	$q[kN/m^3]$	21	10
$h = 15m$	$SF_{\varphi-c}$	1.2016	1.1905
	SF_{Mload}	3.3724	7.3102
Anchored ($c' = 0$)	$q[kN/m^3]$	10	10
$h = 15m$	$SF_{\varphi-c}$	1.1722	1.1069
	SF_{Mload}	6.9482	4.3316
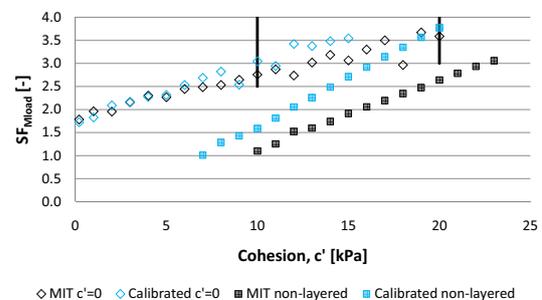
Figure 2: Parametric analysis for the free sheet pile wall. The vertical lines indicate the area in which the two models with $c' = 0$ on the back side provides deviating results.

$20kPa$, marked with black lines in the figure. In the parametric analysis, the cohesion is increased far above this value, and the overall conclusion is a linear variation. The results from this analysis are not illustrated. The deviation for cohesions around $10 - 20kPa$ cannot be explained, and it is assumed that a numerical ill-condition occurs here. Furthermore, these two models were found to be dependent on the input for $\sum M_{load}$, which might explain some of the deviation.

To compare the safety factors of the models, the parametric analysis is conducted with $SF_{\varphi-c}$, cf. Fig. 3. There is a linear dependency with increasing cohesion but the function also reduces φ' and the influence of increasing the cohesion cannot be found from this figure only.

Figure 3: Parametric analysis for the free sheet pile wall.

The cohesions for the two defined materials are different. To be able to compare the results from the non-layered case, it is necessary to create an equal reference. This is done by subtracting the defined cohesion, cf. Tab. 2, from the cohesion used in the model. This implies that 0 on the abscissa refers to the cohesions defined for the original models. 1 refers to the defined cohesion plus one, i.e. $10kPa$ and $14kPa$ for the calibrated and MIT-material, respectively, and so on.

In the non-layered case, the MIT-material is found to have a larger safety factor for the original material settings. This can be explained by the difference in effective cohesion having a larger effect on the ratio than the corresponding difference in internal angle of friction. As the effective cohesion is increased for

both models, the relative difference between the cohesions is decreased, and the difference in the internal angle of friction is of greater influence. When the effective cohesion in both models is increased with more than $2kPa$, the calibrated material provides the largest $SF_{\varphi-c}$.

In the case with $c' = 0$ on the back side to excavation level, the safety factors for the two models are more or less the same. However, when the cohesion in the layer above excavation level on the back side is increased to values above $6kPa$, the calibrated material provides the largest $SF_{\varphi-c}$. It is not possible to compare the non-layered case to the case with $c' = 0$ on the back side to excavation level as the models are constructed with a different height of the wall.

The influence on the maximum bending moment and height of an increasing cohesion is investigated by use of SPOOKS (GEO, 2010), cf. Fig. 4 and 5. Generally, the height is found to decrease linearly with an increasing cohesion, and the maximum bending moment is found to decrease with a polynomial.

Normal Danish practice is to estimate the effective cohesion as 10% of the undrained shear strength. The undrained shear strength is found by Iversen et al. (2010) as an average to $c_{u,k} = 100.8kPa$, and $c'_{10\%,k}$ is calculated to be $10.1kPa$. Introducing the partial coefficient for the drained shear strength reduces the value to $c'_{10\%,d} = 8.4kPa$. This strength is marked with a vertical black line in the figures. Furthermore, this value corresponds approximately to the cohesions found for both the MIT- and the calibrated material.

Applying an effective strength on the back side of the sheet pile wall of $c'_{10\%,d}$ instead of $0kPa$ implies a reduction in the maximum bending moment. In the studied case where Aalborg Clay is used, the reduction on the moment is approximately 83% for the non-layered case and 74% for the case with $c' = 0$ on the back side to excavation level, cf. Tab. 5. The case study shows that the height can be reduced with 20% and 35% for the case with $c' = 0$ on the back side to excavation
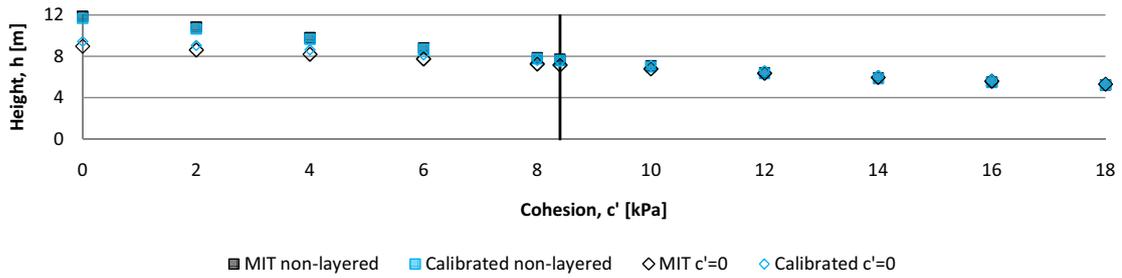
Figure 4: Parametric analysis of the height for the free sheet pile wall. The vertical black line indicates $c'_{10\%,d}$.
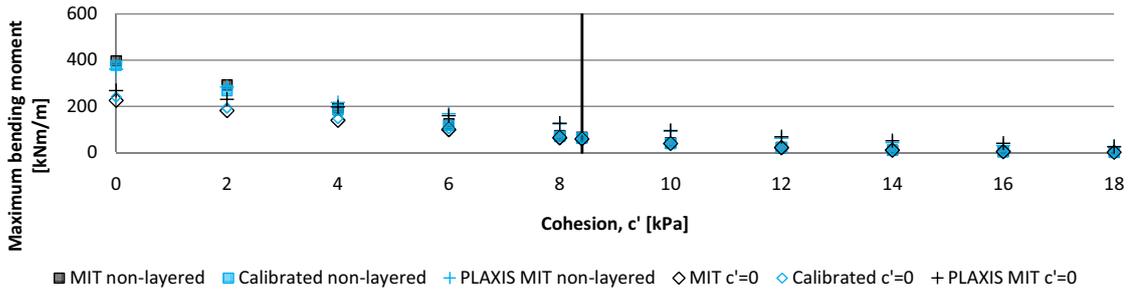
Figure 5: Parametric analysis of the maximum bending moment for a free sheet pile wall. The vertical black line indicates $c'_{10\%,d}$.

level and the non-layered case, respectively.

The maximum bending moment is also calculated by means of PLAXIS, applying the height found by SPOOKS for the corresponding cohesion to each model. The bending moments are generally found to be smaller compared to those found by SPOOKS, but the tendency with a polynomial decrease in the bending moment is the same.

The corresponding analyses are made for an anchored sheet pile wall. The anchor is pre-stressed to $200kN/m$. The first parametric analysis is made with SF_{Mload}, cf. Fig. 6. This analysis shows a linear variation of SF_{Mload} with the cohesion as found for the free sheet pile wall.

For comparison of the two materials, the analysis is made with $SF_{\varphi-c}$, cf. Fig. 7. As for the free sheet pile wall, the abscissa is changed for the non-layered case, and 0 refers to the reference cohesion defined by Iversen et al. (2010). Furthermore, $SF_{\varphi-c}$ is adjusted to 1.2 for the original material settings.

$SF_{\varphi-c}$ obtained for the two materials are equal in the case with $c' = 0$ on the back side
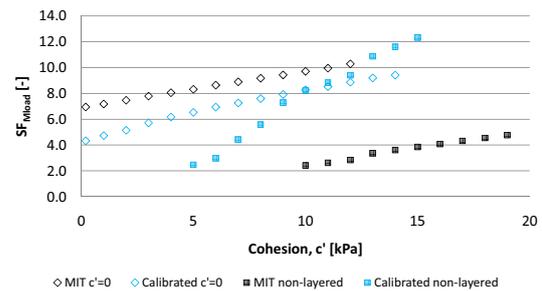
Figure 6: Parametric analysis on SF_{Mload} for the free sheet pile wall.
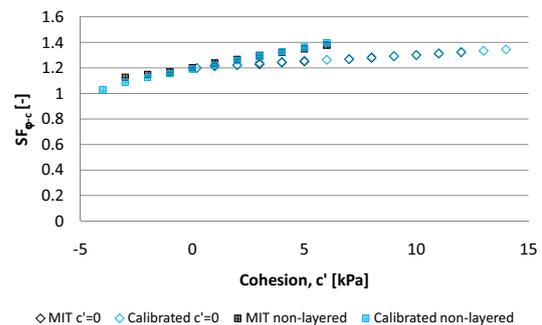
Figure 7: Parametric analysis on $SF_{\varphi-c}$ for the free sheet pile wall.

to excavation level. This indicates that the magnitude of the cohesion in the layers below excavation level is of minor importance for $SF_{\varphi-c}$ of anchored sheet pile walls.

Table 5: Results from the parametric analysis in SPOOKS. Aalborg Clay is used as a case material, and the results only reflect the decrease found for this material. The difference indicates how much the maximum bending moment, height, and anchor force can be lowered if an effective cohesion of $c'_{10\%}$ is applied on the back side compared to using $c' = 0$.

			Difference
Free wall	Non-layered	Maximum bending moment	83%
		Height	35%
	$c' = 0$	Maximum bending moment	74%
		Height	20%
Anchored wall	Non-layered	Maximum bending moment	67%
		Height	14%
		Anchor force	29%
	$c' = 0$	Maximum bending moment	57%
		Height	5%
		Anchor force	21%
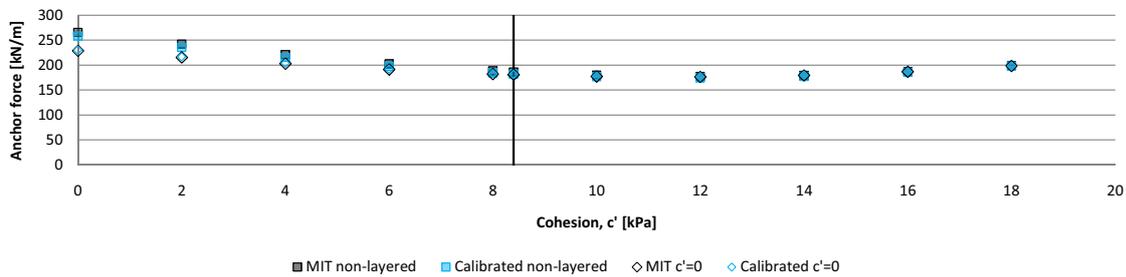
Figure 8: Parametric analysis of the anchor force for an anchored sheet pile wall. The vertical black line indicates $c'_{10\%,d}$.

A small difference is found in the case with non-layered soil where the MIT-material is found to provide a larger safety factor for cohesions equal to or lower than the reference cohesion. For cohesions higher than the reference cohesion, the calibrated material provides the largest $SF_{\varphi-c}$. As for the free sheet pile wall, this difference can be explained by the relative difference between the effective cohesions decreasing as the cohesions are increased. This makes the internal angle of friction more important for the strength.

The practical meaning of an increased cohesion is investigated by SPOOKS for the anchor force, maximum bending moment and height, cf. Fig. 8, 9, and 10, respectively. The vertical black line indicates $c'_{10\%,d} = 8.4kPa$. In SPOOKS several failure mechanisms can be chosen. Here, the failure mechanism corresponding to one yield hinge is chosen (Ovesen et al., 2007).

The effect of the increased cohesion is found to be largest for the maximum bending moment when the cohesion is increased from zero. The case study using Aalborg Clay shows that applying an effective cohesion of $c'_{10\%} = 8.4kPa$ lowers the maximum bending moment with 57% and 67% for the case with $c' = 0$ on back side and non-layered case, respectively, cf. Tab. 5. For the anchor force the reduction is found to $21 - 30\%$, lowest for the case with $c' = 0$ on the back side to excavation level. The height can be reduced by $5 - 14\%$, lowest for the case with $c' = 0$ on the back side to excavation level.

The maximum bending moment in the sheet pile wall in Aalborg Clay is also found by means of PLAXIS. The model is constructed with the height found by SPOOKS for the corresponding cohesion. The progress of the maximum bending moment with increasing cohesion is still found to be polynomial, however, with a much smaller curvature, and the benefit of increasing the cohesion is not as pronounced as found by means of SPOOKS.
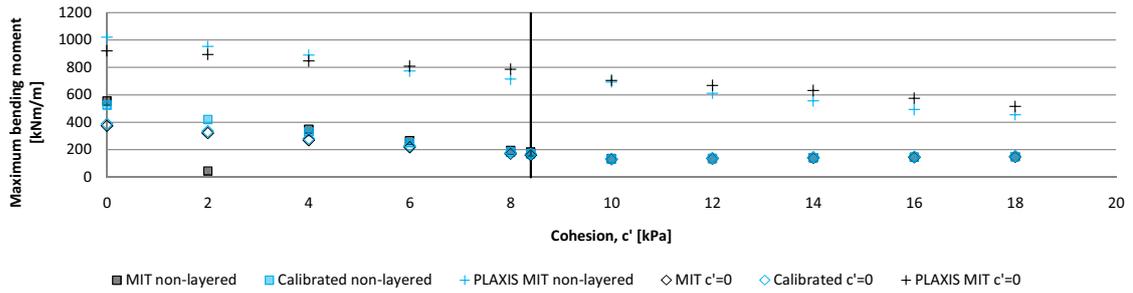
Figure 9: Parametric analysis of the maximum bending moment for an anchored sheet pile wall. The vertical black line indicates $c'_{10\%,d}$.
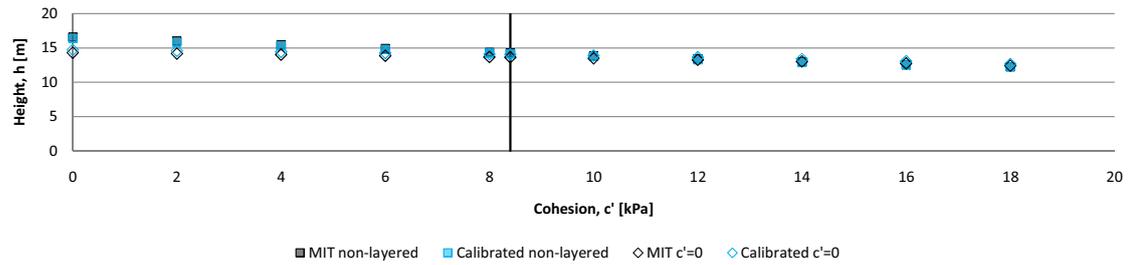
Figure 10: Parametric analysis of the height for an anchored sheet pile wall. The vertical black line indicates $c'_{10\%,d}$.

4   Discussion of Results

The case study shows that the safety factors, defined as the surface load to the critical surface load, increase linearly when the effective cohesion is increased, both for free and anchored sheet pile walls, and both for layered and non-layered stratifications. The analysis is only conducted for cohesions near the cohesion for the original model, i.e. $9kPa$ and $13kPa$ for the non-layered models, and cohesions between $0kPa$ and $15kPa$ in the case with $c' = 0$ on the back side to excavation level. This approach is chosen as PLAXIS previously in these analyses has shown to be unstable in evaluation of the safety factor for constructions far from failure.

In one case (free sheet pile wall with $c' = 0$ on the back side to excavation level) the cohesion is increased from zero to $80kPa$ in the parametric analysis on SF_{Mload}. This analysis shows linear variation between the safety factor and the cohesion in the entire interval, indicating that the linear variation applies even when the cohesion is increased high above the material settings for the original model.

The linear variation indicates that SF_{Mload} of a structure will increase with increasing cohesion.

$SF_{\varphi-c}$ calculated for the two different materials are approximately the same. However, for cohesions decreased below the reference value, the MIT-material has a higher $SF_{\varphi-c}$ as a higher effective cohesion provides a larger effect on $SF_{\varphi-c}$ compared to difference in the internal angle of friction. When the cohesion is increased above the reference value, the calibrated material provides a larger safety factor as the cohesion is of minor importance for $SF_{\varphi-c}$ and a larger internal angle of friction provides a stronger material.

The difference between the internal angles of friction for the two materials are calculated to 2.1%, and the MIT-material has the lowest internal angle of friction. To counterbalance the difference in the internal angle of friction, the cohesion must be $27 - 30\%$ higher to obtain the same safety factor. For differences in the cohesion higher than $27 - 30\%$, the MIT-material has the largest $SF_{\varphi-c}$, while the calibrated material has a larger $SF_{\varphi-c}$ for lower differences.

Furthermore, analyses in SPOOKS show that the height decreases linearly with increasing effective cohesion. For both a free and an anchored wall, the maximum bending moment decreases with a polynomial. This implies that the drop in maximum bending moment is largest when the cohesion is raised from zero to $c'_{10\%}$. Hereafter, the decrease is not distinct. For an anchored sheet pile wall the anchor force also decreases as a polynomial.

Seen from a financial perspective, large savings can be made by investigating whether an effective cohesion of $c'_{10\%}$ can be applied instead of choosing the conservative value and use $c' = 0kPa$ on the back side of the wall to excavation level. This could for instance be the case if the depth of tension cracks was investigated further, and $c' = 0kPa$ only was applied on the part where these tension cracks were present. However, precision adjustment of $1 - 2kPa$ of effective cohesions above $c'_{10\%}$ is of minor importance for the cost of a sheet pile wall as neither the height, the maximum bending moment, nor the anchor force can be lowered particularly.

The parametric analyses on free and anchored sheet pile walls show that the safety factor increases linearly with increasing cohesion for both material definitions. This linear variation is generally found by varying the cohesion around the original cohesion, i.e. from $0kPa$ to $20kPa$. However, in one analysis the cohesion is increased up to $80kPa$, showing linear variation in the entire interval.

The practical meaning of increased effective cohesion is investigated by means of SPOOKS, and it is found that the height of sheet pile walls decreases linearly with increasing cohesion, while both the maximum bending moment and the anchor force for anchored walls decrease with a polynomial. The decrease is found to be the largest for small effective cohesions, and the maximum bending moment can be decreased by up to 84% if the cohesion is raised from $0kPa$ to $c'_{10\%}$. However, for cohesions larger than $c'_{10\%}$ the benefit in lowering the height, bending moment, or anchor force from adjusting the cohesion is smaller. Effort should not be put into smaller adjustments of the cohesion if it is already found to be larger than 10% of c_u.

5 Conclusions

For the models with $c' = 0$ on the back side of the wall, equal values of $SF_{\varphi-c}$ are obtained for the two materials both for a free and an anchored sheet pile wall. Comparing $SF_{\varphi-c}$ calculated for the non-layered case shows that the MIT-material provides a higher safety factor in the original definition. Decreasing the cohesion for both materials still provides the highest safety factor for the MIT-material, while an increase in the cohesion for both materials will provide higher safety factors for the calibrated material.

The difference between the internal angles of friction is 2.1%, which for the MIT-material must be counterbalanced by a $27 - 30\%$ larger cohesion to keep the MIT-material with the largest $SF_{\varphi-c}$.

Bibliography

Brinkgreve, R. B. J. (2008). PLAXIS *2D, Reference Manual, Version 9.0*. PLAXIS b.v.

Dansk Ingeniørforening (1984). *DS415:1984*. Dansk Standard.

European Committee for Standardization (2008). *National Annex to Eurocode 7: Geotechnical design - Part 1: General rules*. Dansk Standard.

GEO (2010, May). Beskrivelse af SPOOKS. On the WWW. URL http://www.geo.dk/forside/ydelser/ geoteknik/designafspunsvægge- spooks/beskrivelseafspooks.aspx.

Iversen, K. M., B. N. Nielsen, and A. H.
Augustesen (2010). Strength properties of
Aalborg Clay.

Lade, P. V. (2003). *Opførsel af konstitutiv
modellering af jord*. Noter for K-8 kursus.
Aalborg University.

Ovesen, N. K., L. Fuglsang, and G. Bagge
(2007). *Lærebog i Geoteknik* (1 ed.).
Polyteknisk Forlag.

PLAXIS b.v. (2010, May). PLAXIS- products
- PLAXIS 2d v9. On the WWW. URL
http://www.plaxis.nl/shop/5/info//
PLAXIS+2D+V9/.

Recent publications in the DCE Technical Report Series

Iversen, K. M., Augustesen, A. H., & Nielsen, B. N. (2010). Vertical Equilibrium of Sheet Pile Walls with Emphasis on Toe Capacity and Plugging. *DCE Technical Report , 94*.

Iversen, K. M., Nielsen, B. N., & Augustesen, A. H. (2010). Strength Properties of Aalborg Clay. *DCE Technical Report , 92*.